DLVO Interaction between Colloidal Particles: Beyond Derjaguin's Approximation

Subir Bhattacharjee,[a] *Menachem Elimelech,*[a,*] *and Michal Borkovec*[b]

[a]*Department of Chemical Engineering, Yale University, 9 Hillhouse Avenue, New Haven, CT, 06520-8286, USA*

[b]*Department of Chemistry, Clarkson University, Potsdam, NY, 13699, USA*

Van der Waals and electrostatic double layer interactions between two colloidal particles are evaluated from the corresponding interaction energies per unit area between two infinite flat plates using a recently developed technique, the surface element integration. Application of the technique to two interacting spheres results in predictions of interaction energies that are substantially more accurate compared to the predictions based on conventional Derjaguin's approximation. The superior results of the technique compared to Derjaguin's approximation are attributed to the more rigorous consideration of particle curvature effects in the surface element integration technique.

INTRODUCTION

Colloidal interactions formulated on the basis of the DLVO (Derjaguin-Landau-Verwey-Overbeek) theory[1,2] are frequently invoked to investigate a vast array of natural and engineered phenomena, such as particle aggregation,[3,4] heterocoagulation,[5–8] colloid deposition,[4,9] and a host of processes involving colloidal stability and transport.[3,4,10] Application of DLVO theory to small colloidal particles may, however, lead to anomalous predictions of the interaction energy, and consequently, the properties of systems involving

such particles. Preponderance of several explanations for such anomalies – for instance, presence of non-DLVO interactions,[10,11] modification of the range of the interactions,[12,13] and presence of surface chemical and morphological heterogeneities[14,15] – have often led to an oversight of the influence of particle curvature and shape on colloidal interactions.

The DLVO interaction energy for a system of like-charged colloidal particles comprises an attractive van der Waals interaction and a repulsive electrostatic double layer interaction. In typical colloidal dispersions, the particle sizes and the separation distances of interest are often larger than the range of these interactions. The effects of particle curvature may be neglected for such systems, thus simplifying the procedure of evaluating the interaction energy. Consequently, many common analytical expressions for the interaction energy between large colloidal particles consider curvature effects only to the leading order. One such well-known procedure leading to several analytical expressions for the interaction energy is Derjaguin's approximation.[16,17] The analytical expressions for the interaction energy based on this technique, which are often remarkably accurate for large particles, may, however, yield erroneous predictions of the interaction energy when the colloidal particles become very small. Barring a few studies that attempt to improve these analytical results by considering the particle curvature effects more rigorously,[8,18–20] it is generally accepted that detailed numerical techniques must be invoked to determine the interaction energy between colloidal particles accurately.

Recently, the rationale of improving the Derjaguin approximation technique was described by systematically analyzing and eliminating some of its debilitating assumptions.[21–23] Based on these principles, an improved scaling technique, the surface element integration (SEI), was developed. This technique rigorously considers the effects of particle curvature and shape. Application of the technique to the sphere - flat plate geometry results in remarkably accurate predictions of the interaction energy.[21]

Here, we extend the surface element integration technique, enabling evaluation of the interaction energy between two curved surfaces, and assess the accuracy of the technique *vis-a-vis* conventional Derjaguin's approximation. The paper is organized as follows. First, we analyze the assumptions in Derjaguin's approximation (DA) leading to its approximate predictions, and point out how SEI corrects some of these approximations. A general formalism for evaluation of the interaction energy between two particles from the corresponding interaction energy per unit area between infinite flat plates is also presented. Following this, the approximations inherent in SEI and DA techniques are analyzed with a specific example of unretarded van der Waals interaction between two spherical particles. Finally, we deal

with the prediction of electrostatic double layer interaction energy using SEI. The paper is concluded with a few remarks regarding our key observations.

SURFACE ELEMENT INTEGRATION FOR TWO CURVED SURFACES

In this section, the primary assumptions in DA, which render the technique approximate, are described. Following this, the mathematical formulation of SEI is presented, highlighting how the assumptions in DA can be avoided for the particle - flat plate geometry to yield extremely accurate results for the interaction energy. Finally, a general formulation for evaluating the interaction energy between two particles from the corresponding interaction energy per unit area between two infinite flat plates is presented.

Assumptions in Derjaguin's Approximation

The Derjaguin approximation (DA) procedure relates the interaction energy per unit area between two flat plates E and the interaction energy between two curved surfaces U by[16,17]

$$U(D) \approx \int_A E(h) \mathrm{d}A \approx f([a_1],[a_2]) \int_D^\infty E(h) \mathrm{d}h \qquad (1)$$

Here, D is the distance of closest approach between the two curved surfaces, $E(h)$ is the interaction energy per unit area between two infinite flat plates separated by a distance h, $\mathrm{d}A$ is the differential area of the surfaces facing each other, $[a_1]$ and $[a_2]$ represent the sets of the two principal radii of curvature of surfaces 1 and 2, respectively, at the distance of closest approach, and $f([a_1],[a_2])$ is a function of the radii of curvature of the surfaces. One should note that for a spherical particle the two principal radii of curvature are identical.

Two assumptions lead to the final expression in Eq. (1).[16,17,21–23] First, the range of the interaction energy is considered much shorter than the radii of curvature of the particles. This implies that the entire interaction energy between the two particles arises from a small region of the particles in the vicinity of the distance of closest approach, thus enabling the extension of the upper integration limit in Eq. (1) to infinity.[3,17] Furthermore, this assumption allows us to neglect higher order curvature effects in writing the final form of Eq. (1).[17,21,22] Consequently, the function $f([a_1],[a_2])$ represents curvature effects that are valid only near the distance of closest approach.[3,16–18]

The second assumption underlying DA is related to the interpretation of the interaction energy per unit area between two infinite flat plates. The interaction energy per unit area is ideally defined as the interaction energy at any point on one of the flat surfaces due to the entire second flat plate.[21] When using DA for two curved surfaces, the interaction energy per unit area between two infinite flat plates is conveniently defined as the interaction energy between two similar area elements on the opposing plates directly facing each other.[10,17–19] This interpretation of interaction energy per unit area leads to an overestimation of the interaction energy between two particles, as will be shown shortly.

Surface Element Integration

The ideal interpretation of the interaction energy per unit area between two infinite flat plates is recovered when dealing with the specific geometry of a particle interacting with an infinite flat plate.[21] In this case, the interaction energy of a differential area element dS on the particle surface arises due to the entire infinite flat plate. For this particular geometry, we can rigorously incorporate the particle curvature in the interaction energy scaling process. Integration of the differential interaction energy of every area element over the exact particle surface leads to the final expression for the total interaction energy between a particle and an infinite flat plate[21]

$$U(D) = \int_{S} \boldsymbol{n} \cdot \boldsymbol{k} \, E(h) \mathrm{d}S = \int_{A} E(h) \frac{\boldsymbol{n} \cdot \boldsymbol{k}}{|\boldsymbol{n} \cdot \boldsymbol{k}|} \mathrm{d}A \qquad (2)$$

where $\boldsymbol{n}$ is the outward unit normal vector on the surface element dS and $\boldsymbol{k}$ is a unit vector normal to the flat plate (directed along the positive z axis). The last expression in Eq. (2) is obtained by projecting the surface of the particle S on a plane parallel to the infinite flat plate.[21] In other words, the area A is a projection of the actual curved surface of the particle on a plane facing the infinite flat plate. It is however important to note that the first integral in Eq. (2) is evaluated over the closed surface S of the particle, which implies that the quantity $\boldsymbol{n} \cdot \boldsymbol{k}$ can assume both positive and negative values.

Assumptions Used in Interaction Energy Scaling

It should be noted that either additional information or some assumptions regarding the decay behavior of the interaction energy are necessary when mapping the interaction energy per unit area between two flat plates to the interaction energy between a particle and a flat plate. In deriving the

surface element integral (Eq. (2)), it was assumed that the interaction force per unit area acts normal to the particle surface.[21] This is an underlying assumption in DA as well. Fortunately, the forces indeed act normal to the particle surface for van der Waals interaction and electrostatic double layer interaction at constant surface potential.[21] For these interactions, Eq. (2) provides very accurate scaling for the sphere – flat plate geometry. However, for double layer interaction at constant surface charge, the stress does not necessarily act normal to the particle surface, and hence, surface element integration cannot give accurate results based on the interaction energy per unit area alone.

Similarly, mapping the interaction energy for two particles (both having curved surfaces) requires additional information about the decay behavior of the interaction energy. In absence of such information, some assumptions regarding the interaction energy become essential. Here, we describe the additional assumption made in such circumstances, and show its consequences when determining the interaction energy.

Consider an infinite flat plate at a distance D from the surface of an infinite cylindrical half-space of radius a, as shown in Figure 1. Let the interaction energy between the half-space and the infinite flat plate be $U(D)$. This implies that the total interaction energy felt by the infinite flat plate due to the cylindrical half-space is $U(D)$ as well. However, the interaction energy is not entirely confined to a circular cylindrical region of the flat plate that is
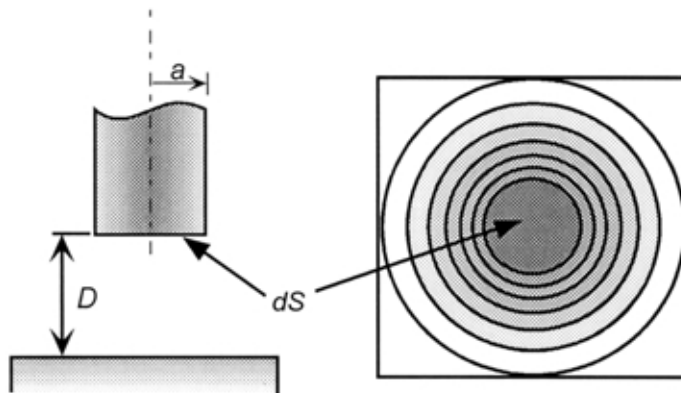

Figure 1. Schematic representation of a cylindrical half-space of radius a (with dS being the area of the circular face) interacting with an infinite flat plate located at a distance D. The geometrical considerations are shown on the left, while the corresponding energy density on the surface of the flat plate is shown on the right. The shaded contours in the right hand side figure represent the radial decay behavior of the interaction energy on the surface of the plate.

identical to the cylindrical half-space. Rather, the interaction energy origi-
nates from a larger region of the infinite flat plate, with a non-uniform en-
ergy density (interaction energy per unit area). The energy density is maxi-
mum near the distance of closest approach between the cylinder and the flat
plate, and decays radially outward (the decay behavior is schematically
shown by the shaded concentric circles in Figure 1).

The above decay behavior should also be observed when considering the
interaction energy between a differential area element on the particle and
the infinite flat plate. If the interaction is short ranged, and in the limit
when the surface element tends to a point ($dS \rightarrow 0$), the radial decay behav-
ior of the energy density on the flat plate may be approximated as a delta
function with its center located directly in front of the surface element. In
other words, a surface element will interact with another element directly
facing it with an intensity $E(h)$, where h is the separation distance between
the elements. Derjaguin's technique for two particles is based on this inter-
pretation of interaction energy per unit area. We note that this assumption
will become progressively inaccurate as the range of the interaction energy
becomes larger. Furthermore, the approximation results in an overestima-
tion of the interaction energy between two surface elements facing each
other as we assume the entire interaction due to a larger area of the plate to
be confined within a small area element of the plate.

In absence of any additional information regarding the interaction en-
ergy, there are practically no other means of further progress without the
above assumption. However, using this assumption in SEI provides an up-
per bound of the interaction energy that is considerably more accurate com-
pared to DA. It is important to note that despite its approximate nature, the
simplicity of DA has led to its widespread use in evaluation of the DLVO in-
teraction energy. Furthermore, in several circumstances involving complex
geometries, DA might be the only feasible computational technique that can
be used to evaluate the interaction energy. Similar arguments can be used
in favor of SEI. While it involves a marginal increase in computational ef-
forts compared to DA, it provides an immense improvement in the interac-
tion energy prediction.

Application of SEI for Two Curved Surfaces

Consider two colloidal particles 1 and 2 facing each other as shown in
Figure 2. The origins of these particles are located at O_1 and O_2. The body
fixed coordinate system for each particle is selected in such a manner that
their xy planes are mutually parallel, while their z axes face each other. In
this system, the planes x_1y_1 and x_2y_2 are separated by a distance H. The
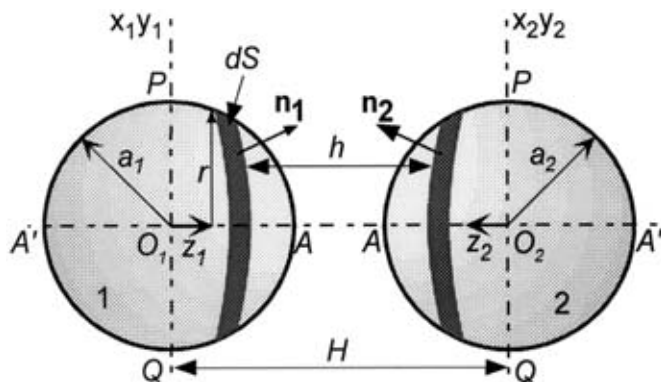equations of the two surfaces may be written as

Figure 2. Schematic representation of two interacting spherical particles of radius a_1 and a_2. The centers of the spheres 1 and 2 are origins of two body-fixed coordinate systems, with their z axes directly facing each other. The xy planes of these coordinate systems are parallel to each other. Differential area elements on the surfaces of the particles are represented by dS. The outward unit normals to the particle surfaces at these differential elements are denoted by $\boldsymbol{n}_1$ and $\boldsymbol{n}_2$. The distance between the origins O_1 and O_2 is H. For radially symmetric particles, the geometry can be conveniently described using cylindrical coordinates (r, z). The surface of each particle is bound by a convex and a concave surface, denoted by PAQ and $PA'Q$, respectively.

$$z_1 = \Im_1(x, y) \tag{3a}$$

and

$$z_2 = \Im_2(x, y), \tag{3b}$$

while the local distance h between the two surfaces at any given (x,y) is

$$h = H - \Im_1(x, y) - \Im_2(x, y). \tag{4}$$

It should be noted that for the closed particle surfaces, the functions $\Im_1(x, y)$ and $\Im_2(x, y)$ are multi-valued, as will be shown shortly for the specific case of spherical particles.

The curved surfaces of the particles 1 and 2 can be considered as made up of numerous differential surface elements of area dS. Each pair of these surface elements on the two surfaces facing each other is assumed to possess a differential interaction energy given by

$$dU \approx (\boldsymbol{n}_1 \cdot \boldsymbol{k}_1)(\boldsymbol{n}_2 \cdot \boldsymbol{k}_2)E(h)dS, \tag{5}$$

where the magnitude of the differential interaction energy is governed by the separation distance h. In this equation, the vectors $\boldsymbol{n}_1$ and $\boldsymbol{n}_2$ represent the outward unit normals to the surfaces, and $\boldsymbol{k}_1$ and $\boldsymbol{k}_2$ represent the unit vectors directed towards the positive z axes of each body-fixed coordinate system. The separation between the two surface elements facing each other is governed by Eq. (4).

Summation of the differential interaction energy over all such pairs of interacting surface elements constituting the two curved surfaces will give the total interaction energy between particles 1 and 2. This interaction energy can be expressed as

$$U = \int_{S_1} dU = \int_{A_1} \boldsymbol{n}_2 \cdot \boldsymbol{k}_2 \, \frac{\boldsymbol{n}_1 \cdot \boldsymbol{k}_1}{|\boldsymbol{n}_1 \cdot \boldsymbol{k}_1|} E(h) dA_1. \tag{6}$$

Here, the first integration is performed over the actual surface of particle 1, while the second integration is performed over the projected area of particle 1 on the xy plane, denoted by A_1.

It should be noted that Eq. (5) is an approximate expression for the interaction energy between two surface elements based on the assumption of pairwise interaction between two surface elements facing each other. The error involved in this assumption will be small only when the interaction energy is very short ranged. This assumption constitutes the basic limitation of both DA and SEI when considering two curved surfaces. It is clear that whenever this assumption fails, the interaction energy predicted by DA or SEI will be greater than the actual interaction energy.

Application of SEI for Two Spherical Particles

Utilizing the radial symmetry of the spherical geometry, we can use cylindrical coordinates and considerably simplify the problem. Considering circular elements on the surfaces of the spheres (see Figure 2), the distance between two elements on the spheres facing each other is

$$h = H \mp a_1 \sqrt{1 - r^2/a_1^2} \mp a_2 \sqrt{1 - r^2/a_2^2} \tag{7}$$

where H is the distance between the centers of the two spheres and a_1 and a_2 are the radii of the spheres. The signs in the above equation are negative or positive, depending on which hemispheres of the spheres 1 and 2 are considered. For instance, when the hemispheres *PAQ* on both the spheres (Figure 2) are considered, both the signs in Eq. (7) are negative.

Each spherical volume is bound by two hemispherical surfaces (shown as *PAQ* and *PA'Q* in Figure 2). From Eq. (6) we note that the quantity $n_1 \cdot k_1$ / $|n_1 \cdot k_1|$ will assume a value of +1 or –1 depending on whether $n_1 \cdot k_1$ is positive or negative. The term $n_1 \cdot k_1$ represents the cosine of the angle that the unit outward normal to the surface makes with the positive z axis. It is evident that for spherical surfaces, when we consider the hemisphere *PAQ*, this quantity will be positive, while for hemisphere *PA'Q*, it will be negative. Furthermore, the term $n_2 \cdot k_2$ will also assume positive and negative values on hemispheres *PAQ* and *PA'Q* of the second sphere. Therefore, in case of two spheres, a total of four interaction energy terms are obtained. Each hemispherical surface of sphere 2 (*PAQ* and *PA'Q*) interacts with two hemispherical surfaces of sphere 1. Thus, when determining the interaction energy between spheres 1 and 2, the interaction energy of sphere 1 due to the surface *PAQ* of sphere 2 is obtained first. This requires the evaluation of two interaction energy terms, U_{12}^{AA} and $U_{12}^{A'A}$, where the subscripts 1 and 2 refer to the spheres considered and the superscripts A and A' refer to the hemispheres *PAQ* and *PA'Q*, respectively. Following this, the interaction energy between sphere 1 and the hemisphere *PA'Q* of sphere 2 is determined. The two interaction energy terms needed for this step are $U_{12}^{AA'}$ and $U_{12}^{A'A'}$. Finally, the total interaction energy between the two spheres is obtained by adding all the four interaction energy terms, yielding

$$U(H) = U_{12}^{AA} - U_{12}^{A'A} - U_{12}^{AA'} + U_{12}^{A'A'} \tag{8}$$

where $U(H)$ is the total interaction energy between the two particles with center to center separation H.

The signs preceding the interaction energy terms in Eq. (8) arise from the different combinations of the signs of $n_1 \cdot k_1$ and $n_2 \cdot k_2$. Writing Eq. (6) in cylindrical coordinates, the four interaction energy terms used in Eq. (8) assume the following explicit forms

$$U_{12}^{AA} = 2\pi \int_0^{a_1} \left(\sqrt{1 - r^2/a_2^2} \right) E\left[H - a_1\sqrt{1 - r^2/a_1^2} - a_2\sqrt{1 - r^2/a_2^2} \right] r\,dr$$

$$U_{12}^{A'A} = 2\pi \int_0^{a_1} \left(\sqrt{1 - r^2/a_2^2} \right) E\left[H + a_1\sqrt{1 - r^2/a_1^2} - a_2\sqrt{1 - r^2/a_2^2} \right] r\,dr$$

$$\tag{9}$$

$$U_{12}^{AA'} = 2\pi \int_0^{a_1} \left(\sqrt{1 - r^2/a_2^2} \right) E\left[H - a_1\sqrt{1 - r^2/a_1^2} + a_2\sqrt{1 - r^2/a_2^2} \right] r\,dr$$

$$U_{12}^{A'A'} = 2\pi \int_0^{a_1} \left(\sqrt{1 - r^2/a_2^2} \right) E\left[H + a_1\sqrt{1 - r^2/a_1^2} + a_2\sqrt{1 - r^2/a_2^2} \right] r\,dr$$

The term $\sqrt{1 - r^2/a_2^2}$ in the above integrals represents $|\mathbf{n_2} \cdot \mathbf{k_2}|$. The terms in the square brackets arise from the four possible combinations of signs in Eq. (7). Equation (9) implies that four integrals need to be evaluated to obtain the interaction energy, each of which is evaluated over a pair of hemispherical surfaces bounding the spherical particles as described earlier. In evaluating the interaction energy using Eq. (9), one should perform the integration over the radius of the smaller particle, *i.e.* $a_1 \leq a_2$. Here, the differential area dA_1 ($= 2 \pi r \, dr$) is the projection of the actual spherical surface element dS_1 on the xy plane.

Although we have considered the curvature of the two spheres, the interaction energy was obtained by assuming pairwise interaction between two surface elements facing each other. This assumption leads to the approximation in the surface element integral. However, consideration of the exact curvature of the surface in SEI renders this technique superior to Derjaguin's approximation over larger separation distances and smaller particle sizes. The influence of both these effects are shown in the next section for the particular case of van der Waals interaction between two spheres.

VAN DER WAALS INTERACTION BETWEEN
TWO SPHERICAL PARTICLES

In this section, the superiority of SEI over DA is demonstrated by considering the example of van der Waals interaction between two spherical particles. The non-retarded van der Waals interaction energy per unit area between two infinite flat plates separated by a distance h is given by[24]

$$E(h) = -\frac{A_H}{12\pi h^2} \, , \tag{10}$$

where A_H is the Hamaker constant of the interacting media. Substituting this in Eq. (9) yields the interaction energy between two spherical particles.

The expression for the non-retarded van der Waals interaction energy between two spherical particles of radii a_1 and a_2 can be obtained using Hamaker's approach[4,24]

$$U_{VDW}^{Hamaker} = -\frac{A_H}{6} \left[\frac{2a_1 a_2}{D^2 + 2a_1 D + 2a_2 D} + \frac{2a_1 a_2}{D^2 + 2a_1 D + 2a_2 D + 4a_1 a_2} \right.$$
$$\left. + \ln\left(\frac{D^2 + 2a_1 D + 2a_2 D}{D^2 + 2a_1 D + 2a_2 D + 4a_1 a_2} \right) \right] \tag{11}$$

where D is the distance of closest approach between the particle surfaces, that is, $D = H - a_1 - a_2$. This expression is used here as a benchmark for comparison of the van der Waals interaction energy predictions obtained using the SEI and DA techniques. The corresponding expression for the interaction energy obtained using DA is[4]

$$U_{\text{VDW}}^{\text{DA}} = -\frac{A_{\text{H}}}{6} \frac{a_1 a_2}{(a_1 + a_2)} \frac{1}{D} \tag{12}$$

Figure 3 compares the ratios of the van der Waals interaction energy obtained using SEI and DA with the prediction given by Eq. (11). It is evident that both SEI (solid lines) and DA (dashed lines) overpredict the interaction energy between two spherical particles, though the agreement between the interaction energy predictions obtained using SEI and Eq. (11) is much better over all separation distances. Furthermore, as the size ratio of the two particles (a_2 / a_1) increases, the predictions based on SEI improve considera-
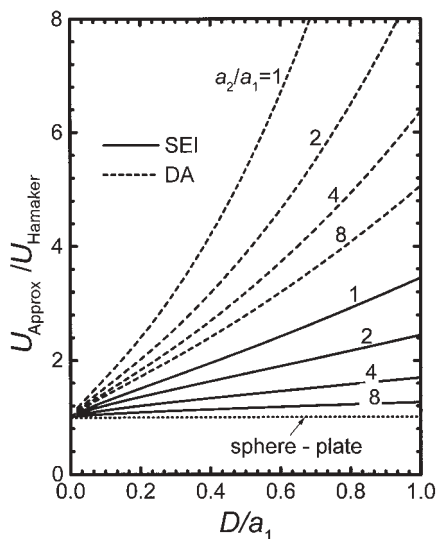

Figure 3. Comparison of the unretarded van der Waals interaction energy between two spheres of different radii obtained using SEI and DA. Variations of the ratio of van der Waals interaction obtained using either of the approximate techniques to the Hamaker result is shown with the scaled separation distance D/a_1 for different size ratios a_2 / a_1. A value of 1 for the interaction energy ratio indicates an exact agreement between the approximate and the Hamaker results (indicated by the horizontal dotted line). This exact agreement is achieved by SEI for the sphere – infinite flat plate geometry. The results shown in the figure are independent of the particle radii.

bly, resulting in exact agreement with the Hamaker expression for the sphere – flat plate geometry ($a_2 \to \infty$). For the sphere – flat plate geometry, SEI and Hamaker's approach provide the same analytical expression for the unretarded van der Waals interaction energy, indicating that SEI provides an exact scaling of the interaction energy in this case.[21]

Although the results presented here are applicable to unretarded van der Waals interaction energy, application of SEI should not be limited to this case alone. The technique can be applied to predict the retarded van der Waals interaction energy between two particles from the corresponding interaction energy per unit area between two infinite flat surfaces. Finally, although the results presented here were derived for the spherical geometry, the technique may be used for arbitrary particle shapes, and hence, may be a more facile substitute of the Hamaker integration approach for evaluation of the VDW interaction energy between colloidal particles of various shapes. An estimate of the accuracy of the technique for various particle geometries can always be obtained by evaluating the interaction energy between a particle and a flat plate, in which case it has been shown that the technique predicts the unretarded VDW interaction energy exactly.[21]

ELECTROSTATIC DOUBLE LAYER INTERACTION BETWEEN SPHERES

In this section, we use SEI to determine the electrostatic double layer (EDL) interaction energy between a sphere and a flat plate at constant surface potential, and compare the results with the corresponding interaction energies predicted by Derjaguin's technique and the linear superposition approximation (LSA). We commence this section with a summary of the various approaches used to determine the interaction energy from the solution of the Poisson-Boltzmann (PB) equation and their limitations. This is followed by a presentation of the explicit forms of the flat-plate interaction energy per unit area used in SEI to determine the interaction energy between two spheres. Finally, the interaction energies predicted by SEI, DA, and the LSA techniques are compared.

Limitations of Available Approaches

The interaction energy and the force between overlapping spherical double layers are generally derived from the corresponding expressions for flat plates using Derjaguin's approximation.[3,4,25] A second approach for determining the interaction energy between spherical particles is based on the linear superposition principle.[26] Both these approaches for obtaining the in-

teraction energy between two spherical particles are approximate as they either neglect higher order curvature effects, or assume non-overlapping double layers. While DA is likely to be accurate at short separation distances, the linear superposition results are considered more appropriate at large separations or for thin double layers.[18,26,27]

More accurate techniques for evaluation of double layer interactions have been developed based on variational, series expansion, and perturbation methods.[18,28–31] In addition, numerical results using finite element, boundary element, and finite difference solutions of the PB equation have been reported.[27,32–35] A major deterrent toward usage of these detailed numerical or series solutions is the considerable computational burden.

Several rigorous numerical and analytical results for the interaction energy between two infinite flat plates based on the solution of the PB equation are available.[25,36] However, one must revert to Derjaguin's approximation to obtain the interaction energy for other particle geometries.[25] When scaling the interaction energy for other particle shapes, the accuracy of the flat plate interaction energy may be completely obscured by the approximations inherent in Derjaguin's technique. Recently, some detailed numerical solutions of the PB equation and the corresponding predictions of the double layer force and interaction energy of spherical particles have been reported.[34,35] Following the behavior of the interaction energy and the force predicted by these studies, it appears that for high electrolyte concentrations, that is, when the double layers are thin, Derjaguin's approximation is reasonably accurate under constant potential conditions. However, at low electrolyte concentrations, the agreement between DA and these numerical results deteriorates substantially. Therefore, the interaction energy obtained using DA should be applied cautiously keeping in mind the domains of validity of such results.

EDL Interaction at Constant Surface Potential

In this (sub)section, predictions of the EDL interaction energy between two spherical particles under constant surface potential based on SEI are presented. A rigorous comparison of the SEI estimates for the interaction energy derived here with some of the more detailed numerical or semi-analytical results is beyond the scope of the present study. Hence, we restrict our comparisons with the most facile analytical expressions commonly used to determine the EDL interactions.

Two expressions for flat-plate interaction energy at constant surface potential are used in SEI. First, SEI was applied to the expression of Hogg *et al.,*[37] which is given by

$$E_{\mathrm{CP,LPB}}(h) = \frac{\varepsilon_0 \varepsilon_\mathrm{r} \kappa}{2} \left[\left(\psi_1{}^2 + \psi_2{}^2 \right) \left\{ 1 - \coth(\kappa h) \right\} + 2\psi_1 \psi_2 \operatorname{cosech}(\kappa h) \right] \quad (13)$$

Here, ε_0 is the permittivity in vacuum, ε_r is the relative dielectric permittivity of the solvent, κ is the inverse Debye screening length, and ψ_1 and ψ_2 are the surface potentials of the two flat surfaces. This expression is valid for small surface potentials (less than 25 mV) and symmetrical electrolytes. The sphere-sphere interaction energy was also obtained from the linear superposition expression for the flat plate interaction energy per unit area[38]

$$E_{\mathrm{CP,LSA}} = 32\varepsilon_0 \varepsilon_\mathrm{r} \kappa \gamma_1 \gamma_2 \left(\frac{kT}{ve} \right)^2 \exp(-\kappa h) \quad (14)$$

where $\gamma_i = \tanh(\Psi_i/4)$, $\Psi_i = ve\,\psi_i/kT$, k is the Boltzmann constant, v is the charge number, e is the electronic charge, and T is the absolute temperature.

To determine the interaction energy between two spheres, the surface element integration is performed by substituting Eq. (13) or (14) in Eq. (9). The sphere-flat plate interaction energies obtained using SEI are compared with the Derjaguin approximation results. Application of DA to Eq. (13) yields[37]

$$U_{\mathrm{CP,LPB}}^{\mathrm{DA}} = \pi\varepsilon_0\varepsilon_\mathrm{r} \frac{a_1 a_2}{(a_1 + a_2)} \left(\frac{kT}{ve} \right)^2 \left(\Psi_1{}^2 + \Psi_2{}^2 \right) \left[\frac{2\Psi_1\Psi_2}{\Psi_1{}^2 + \Psi_2{}^2} \ln\left(\frac{1 + e^{-\kappa D}}{1 - e^{-\kappa D}} \right) \right.$$
$$\left. + \ln\left(1 - e^{-2\kappa D} \right) \right] \quad (15)$$

while using Eq. (14) in DA yields[4,38]

$$U_{\mathrm{CP,LSA}}^{\mathrm{DA}} = 64\pi\varepsilon_0\varepsilon_\mathrm{r} \gamma_1 \gamma_2 \frac{a_1 a_2}{(a_1 + a_2)} \left(\frac{kT}{ve} \right)^2 \exp(-\kappa D) \quad (16)$$

Furthermore, we also compare SEI with the linear superposition expression of Bell *et al.*[26] for the interaction energy between two spheres. This expression, which is known to be accurate for $\kappa D \gg 1$ and $\kappa a \geq 10$ is given by[26]

$$U_{\mathrm{LSA}} = \frac{64\pi\varepsilon_0\varepsilon_\mathrm{r} a_1 a_2}{(D + a_1 + a_2)} \left(\frac{kT}{ve} \right)^2 \gamma_1 \gamma_2 \exp(-\kappa D) \quad (17)$$

The interaction energies obtained by the various techniques are compared in Figures 4 to 7. All the figures were obtained using surface poten-

tials of 25 mV on both the spheres, and by varying the electrolyte (1:1) concentration between 10^{-4} and 10^{-1} mol dm^{-3}. The radius of one of the spheres was fixed as 10 nm. Thus, for two similar spheres, the radii of both spheres was taken to be 10 nm, while for dissimilar spheres, the particle size ratio a_2/a_1 was varied by changing the radius of the larger sphere (a_2) keeping the radius of the smaller sphere (a_1) fixed at 10 nm. In all the figures, variations of the electrostatic double layer interaction energy scaled with respect to kT (corresponding to T = 298 K) are shown with the scaled separation distance κD for different values of the parameter κa. The parameter κa reflects the combined influence of particle size and ionic strength of the electrolyte. For a fixed particle radius, the parameter reflects the change in the electrolyte concentration. For instance, when considering a sphere of radius 10 nm, the parameter κa has a value of about 10 for ionic strength of 10^{-1} mol dm^{-3}, while it has a value of about 0.3 at ionic strength of 10^{-4} mol dm^{-3}.

Figure 4 compares the dimensionless interaction energy, U_{EDL}/kT, obtained using Eq. (13) in SEI and DA for two equal spheres of radius 10 nm. There is a marked difference between the quantitative predictions of the interaction energy using DA and SEI. While the two predictions are in conformity at larger values of the parameter κa, the interaction energy predicted
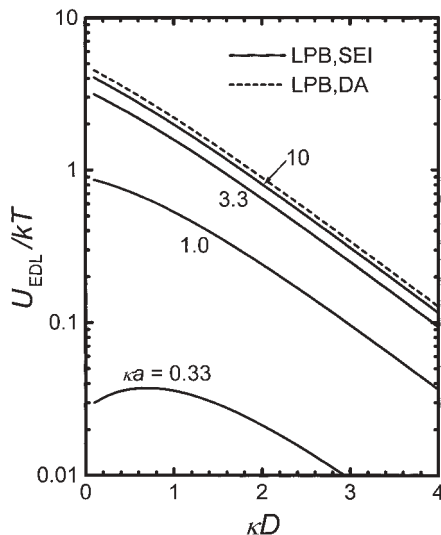

Figure 4. Comparison of the electrostatic double layer (EDL) interaction energy at constant potential between two equal spheres of radii 10 nm obtained by applying SEI and DA to Eq. (13). The variation of the predicted interaction energy with the scaled separation distance κD and the parameter κa are shown. The dimensionless surface potential Ψ (= $ve\psi/kT$) on both the sphere and the flat plate is 1.

using SEI deviates significantly from DA predictions at lower values of κa. It is worth noting that for fixed particle radii, when the interaction energy is presented as a function of the scaled distance κD, DA appears to be insensitive to variations in κa. In sharp contrast, the interaction energy predicted by SEI decreases with decreasing κa, thus signifying an additional dependence on electrolyte concentration.

The corresponding predictions of the interaction energy obtained using Eq. (14) in SEI and DA are depicted in Figure 5. Once again, similar trends are observed as in Figure 4. Since the underlying flat-plate interaction energy expression based on LSA (14) is accurate at large separation distances, the corresponding SEI predictions depicted in Figure 5 should also be accurate at large separations. The predictions based on DA, Eq. (16), however, remain unaffected by variations of the parameter κa. Hence, the interaction energies predicted by SEI at low electrolyte concentrations are substantially lower compared to the predictions of DA.
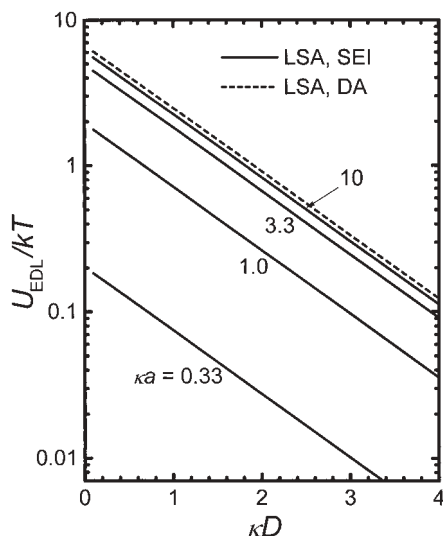

Figure 5. Electrostatic double layer repulsion between two identical spheres of radii 10 nm obtained using Eq. (14) in SEI and DA. All the parameters used are same as in Figure 4.

Figure 6 depicts the interaction energy predictions obtained using Eq. (13) in SEI, and from the well-known LSA expression of Bell *et al.*, Eq. (17) for two equal spheres. Unlike the DA result, Eq. (16), which remains unchanged with variations of κa (see Figure 5), the expression of Bell *et al.* in-
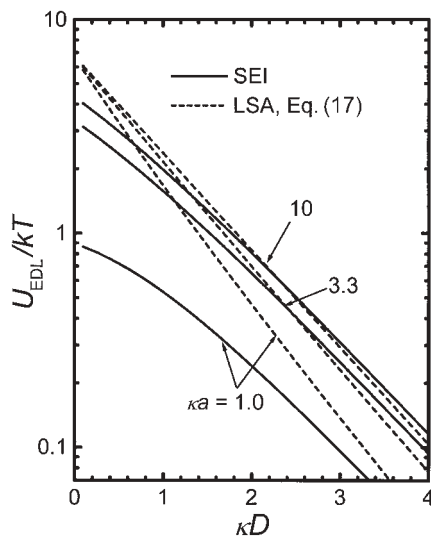
Figure 6. Comparison of the EDL interaction energy between two equal spheres of radii 10 nm predicted by using Eq. (13) in SEI and the linear superposition approximation (LSA) Eq. (17). The dashed lines represent the LSA results. The curves were obtained using a scaled surface potential of 1 on both particles.

deed shows an additional dependence of the interaction energy on κa. It is evident that the agreement between the SEI and the LSA predictions improves at larger κD for all κa. Furthermore, the LSA predictions at large separations become slightly lower than the corresponding SEI predictions, thus confirming our earlier observation that SEI should slightly overpredict the interaction energy because of the inherent assumption of pairwise interaction of surface elements. At small separation distances, LSA is known to be inaccurate and overpredicts the interaction energy considerably for constant potential surfaces.

Finally, Figure 7 provides a rough assessment of the extent of error in SEI for electrostatic double layer interactions. Previously it was shown that SEI provides very accurate results for electrostatic double layer interaction between a sphere and an infinite flat plate under constant surface potential condition.[21] Utilizing this asymptotic limit as a benchmark, the interaction energy between two spheres is determined for various size ratios a_2/a_1. Figure 7 indeed demonstrates that as the size ratio is increased, the SEI predictions for two spheres tend towards the sphere-flat plate interaction energy. Furthermore, the interaction energy for a size ratio of 2 or larger is remarkably close to the sphere-flat plate interaction energy. Thus, the SEI predictions of the interaction energy become very accurate for such dissimilar spheres.
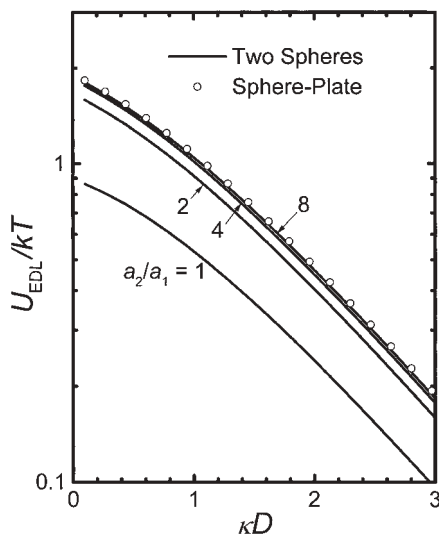
Figure 7. Electrostatic double layer interaction energy for dissimilar spheres predicted using Eq. (13) in SEI. The predictions were obtained by fixing the radius of one sphere as 10 nm, and by varying the radius of the second sphere to yield different values of the ratio a_2/a_1. All the curves were obtained for an electrolyte concentration of 10^{-3} mol dm^{-3} (κa about 1) and scaled surface potentials of 1 on both the particles. The symbols represent the interaction energy between a sphere and an infinite flat plate.

CONCLUDING REMARKS

The surface element integration (SEI) technique can be used to determine the interaction energy between two particles much more accurately than Derjaguin's approximation. Performance of SEI improves for interaction between two spherical particles of different size, and in the limit of sphere-flat plate interaction, the technique becomes very accurate.

Calculation of the electrostatic double layer interaction for constant particle surface potential using SEI suggests that Derjaguin's approximation and the linear superposition approximation for spherical double layers result in gross overestimation of the interaction energy for small particles at low electrolyte concentrations. It is postulated that the vast difference between SEI and existing methods is primarily due to surface curvature effects. Existing methods neglect higher order particle curvature effects, which might result in a marked overestimation of electrostatic double layer interactions for small particles and low ionic strength. The use of the surface element integration technique results in lower repulsive DLVO interaction energies for small particles, particularly at low ionic strengths.

Another important and powerful feature of SEI is its applicability to particles and surfaces of arbitrary geometry. In this study, SEI was used for simple cases of interaction between two spherical particles or between a spherical particle and a flat surface. SEI, however, can be readily applied to obtain the orientation dependent interaction between non-spherical particles, such as ellipsoids, or the interaction between rough surfaces provided the roughness of the surface can be modeled appropriately.

APPENDIX: NOMENCLATURE

a	sphere radius
A	projected area of a curved surface on the xy plane
A_{H}	Hamaker constant
D	distance of closest approach between two surfaces
E	interaction energy per unit area
e	electronic charge
h	distance between two surface elements
H	distance between the origins of two half-spaces
k	Boltzmann constant (1.38×10^{-23} J K^{-1})
$\boldsymbol{k}$	unit normal vector directed towards the positive z axis of a body fixed coordinate system
$\boldsymbol{n}$	unit outward normal vector to the surface
r	radial coordinate in a cylindrical coordinate system
S	actual curved surface of a particle
T	absolute temperature (kelvins)
U	interaction energy between two particles
x, y, z	Cartesian coordinates

Greek Symbols

ε_0	dielectric permittivity in vacuum, 8.8542×10^{-12} C^2/J m (SI units)
ε_{r}	relative dielectric permittivity of solvent (78.54 for water)
Ψ	dimensionless surface potential ($ve\psi/kT$)
κ	inverse Debye screening length
ν	charge number (valence of a electrolyte)
ψ	surface potential

Abbreviations

CP   constant surface potential
DA   Derjaguin's Approximation
DLVO   Derjaguin-Landau-Verwey-Overbeek
EDL   electrostatic double layer
LSA   linear superposition approximation
PB   Poisson-Boltzmann
SEI   surface element integration
VDW   van der Waals

REFERENCES

1. B. V. Derjaguin and L. Landau, *Acta Physicochim*. *(URSS)* **14** (1941) 633–662.
2. E. J. W. Verwey and J. Th. G. Overbeek, *Theory of Stability of Lyophobic Colloids*, Elsevier, Amsterdam, 1948.
3. W. B. Russel, D. A. Saville, and W. R. Schowalter, *Colloidal Dispersions*, Cambridge Univ. Press, Cambridge, 1989.
4. M. Elimelech, J. Gregory, X. Jia, and R. A. Williams, *Particle Deposition and Aggregation*: *Measurement, Modelling and Simulation*, Butterworth-Heinemann, Oxford, 1995.
5. E. Matijević and N. Kallay, *Croat. Chem. Acta* **56** (1983) 649–661.
6. J. E. Kolakowski and E. Matijević, *J. Chem. Soc., Faraday Trans. I*, **75** (1979) 65–78.
7. R. J. Kuo and E. Matijević, *J. Chem. Soc., Faraday Trans. I*, **75** (1979) 2014–2026.
8. H. Kihira and E. Matijević, *Adv. Colloid Interface Sci*. **42** (1992) 1–31.
9. J. N. Ryan and M. Elimelech, *Colloids Surf. A*, **107** (1996) 1–56.
10. J. N. Israelachvili, *Intermolecular and Surface Forces*, 2nd Ed., Academic Press, London, 1992.
11. C. J. van Oss, *Colloids Surf. A,* **78** (1993) 1–49.
12. K. S. Schmitz, *Langmuir* **12** (1996) 3828–3843.
13. P. M. Chaikin, P. Pincus, S. Alexander, and D. Hone, *J. Colloid Interface Sci.* **89** (1982) 555–562.
14. M. Elimelech and C. R. O'Melia, *Langmuir* **6** (1990) 1153–1163.
15. J. Czarnecki, *Adv. Colloid Interface Sci.* **24** (1986) 283–319.
16. B. V. Derjaguin, *Kolloid Z*. **69** (1934) 155–164.
17. L. R. White, *J. Colloid Interface Sci.* **95** (1983) 286–288.
18. A. B. Glendinning and W. B. Russel, *J. Colloid Interface Sci*. **93** (1983) 95–104.
19. K. D. Papadopoulos and H. Y. Cheh, *AIChE. J*. **27** (1984) 7–14.
20. E. Barouch and E. Matijević, *J. Chem. Soc., Faraday Trans. I*, **81** (1985) 1797–1817.
21. S. Bhattacharjee and M. Elimelech, *J. Colloid Interface Sci*. **193** (1997) 273–285.
22. S. Bhattacharjee and A. Sharma, *Langmuir* **12** (1996) 5498–5500.
23. S. Bhattacharjee and A. Sharma, *J. Colloid Interface Sci*. **187** (1997) 83–95.
24. H. C. Hamaker, *Physica* **4** (1937) 1058–1072.

25. D. McCormack, S. L. Carnie, and D. Y. C. Chan, *J. Colloid Interface Sci.* **169** (1995) 177–196.
26. G. M. Bell, S. Levine, and L. N. McCartney, *J. Colloid Interface Sci.* **33** (1970) 335–359.
27. P. Warszynski and Z. Adamczyk, *J. Colloid Interface Sci.* **187** (1997) 283–295.
28. L. R. White, *J. Chem. Soc., Faraday Trans. II*, **73** (1977) 377–396.
29. H. Ohshima, T. W. Healy, and L. R. White, *J. Colloid Interface Sci.* **89** (1982) 484–493.
30. H. Ohshima and T. Kondo, *J. Colloid Interface Sci.* **126** (1988) 382–383.
31. S. L. Carnie, D. Y. C. Chan, and J. S. Gunning, *Langmuir* **10** (1994) 2993–3009.
32. B. K. C. Chan and D. Y. C. Chan, *J. Colloid Interface Sci.* **92** (1983) 281–283.
33. L. N. McCartney and S. Levine, *J. Colloid Interface Sci.* **30** (1969) 345–354.
34. S. L. Carnie, D. Y. C. Chan, and J. Stankovich, *J. Colloid Interface Sci.* **165** (1994) 116–128.
35. M. L. Grant and D. A. Saville, *J. Colloid Interface Sci.* **171** (1995) 35–45.
36. O. F. Devereux and P. L. DeBruyn, *Interaction of Plane Parallel Double Layers*, MIT Press, Cambridge, 1963.
37. R. I. Hogg, T. W. Healy, and D. W. Fuerstenau, *Trans. Faraday Soc.* **62** (1966) 1638–1651.
38. J. Gregory, *J. Colloid Interface Sci.* **51** (1975) 44–51.

SAŽETAK

DLVO-interakcije između koloidnih čestica iznad Derjaguinovih aproksimacija

Subir Bhattacharjee, Menachem Elimelech i Michal Borkovec

Novorazvijena tehnika integriranja površinskih elemenata primijenjena je za računanje van der Waalsovih i elektrostatskih interakcija u električnom međusloju između dvije koloidne čestice. Razmatraju se interakcijske energije po jedinici površine za dvije beskonačne ravne plohe. Taj pristup, primijenjen na dvije sfere, daje znatno pouzdanije rezultate od uobičajene Derjaguinove aproksimacije. Prednost je ove tehnike pred Derjaguinovom aproksimacijom u strožem razmatranju zakrivljenosti.